ELSEVIER

Desalination 128 (2000) 139–145

DESALINATION

www.elsevier.com/locate/desal

Theoretical investigation on the performance prediction of solar still

Berge Djebedjian, Magdy Abou Rayan*

Faculty of Engineering, Mansoura University, 35516 El-Mansoura, Egypt
Tel. +20 (50) 345758; Fax +20 (3) 5970641; E-mail: mrayan@usa.com

Received 22 September 1999; accepted 19 October 1999

Abstract

A theoretical investigation on the performance prediction of solar still is presented in this paper. A solar still of conventional type is considered. The mathematical model is based on time-averaged Navier–Stokes equations. The effect of the variable fluid properties is taken into consideration by using a mixture of air and vapour in the still. A steady state two-dimensional approach with constant temperature boundaries is considered. A discretization schema with finite-difference technique is adapted. The SIMPLER (Semi-Implicit Method for Pressure-Linked Equations Revised) methodology is used. The grid size independence solution is checked for convergence. The numerical results show clearly different zones of circulation with reverse velocity on the inside still glass cover. The numerical results prove the necessity to undertake a numerical investigation before the sizing of solar still. The objective of the present investigation is to present a mathematical model in order to improve the still design, also the obtained results prove to be a good tool for performance prediction according to a given geometry.

Keywords: Numerical analysis; Solar still; Solar desalination; Sea water desalination

1. Introduction

In several regions around the world and particularly the MENA (Middle East North Africa) countries, the water shortage problem presents a real threat to the economic development plants. The rapid growth of population and the increased per capita consumption together with the tremendous urban growth and population reallocation plans have increased the demand for water. In many countries, the desalination is conceived as a non-conventional source of water. The solar desalination is an ideal solution for rural and isolated areas. The solar still is the simplest technology suitable for use in these areas.

* Corresponding author.

Presented at the Fourth International Water Technology Conference IWTC 99, Alexandria, Egypt.

PII: S0011-9164(00)00029-1

The important task is how to improve the poor productivity of these systems. The important factors are the geometry and the glass cover system, in fact both are coupled.

Several experimental and theoretical efforts have been undertaken in this area [5,8]. These studies incorporate the effect of climatic operation, design parameters. The idea of single basin still is based on water diffusion. A maximum distillate yield will result from a minimal air volume contained within the greenhouse envelope [3].

The system is similar to a cavity, the mathematical modelling improves the understanding of flow inside the cavity. This is a step towards the search for ideal cavity geometry that would enhance natural convection.

Palacio and Fernandez [3] studied numerically the flow in a greenhouse-type solar still. They simplified their analysis by means of an equivalent Prandtl number (Pr = 0.1) allowing for the moist air in the inside of the cavity to be represented as a perfect gas.

The effect of the variable fluid properties on laminar free convection heat transfer of monoatomic gas, polyatomic gas, air and water vapour along an isothermal vertical plate has been reported by Shang and Wang [6,7].

In this paper, the thermodynamics of the humid air was used to simulate a real flow in the still. Similar to the solar still explained Tiwari et al. [9], the considered configuration is of a single slope still. Generally, the flow pattern in the solar still is characterised by its aspect ratio H/L and the slope of the glass cover θ. In the present study, the dimensions of the still are similar to those mentioned in Rayan et al. [5]. The basin area of the still (W×L) is 0.5×1 m, the heights of the front and back walls are 0.24 m and 0.5 m, respectively. The glass cover slope is 15°.

The objective of the present investigation is to present a mathematical model capable of predicting the flow characteristics inside the still. The prediction of flow pattern is a first step towards the prediction of solar still performance and hence the configuration optimization.

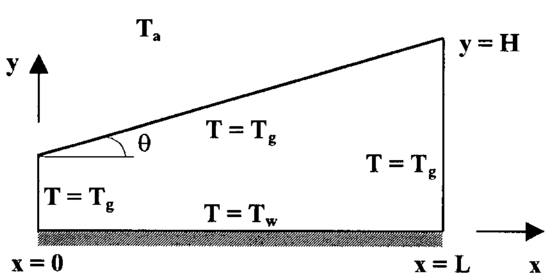

Fig. 1. Basic dimensions of the solar still and the associated boundary conditions.

2. Mathematical formulation

2.1. Governing equations

The present work is based on the numerical solutions of the two-dimensional form of the time-averaged Navier–Stokes equations.

For a variable ϕ, where ϕ may be unity (mass conservation), u and v (momentum conservation) and T (Temperature conservation), etc., the conservative form of the ϕ-conservation equation for the steady two-dimensional incompressible flow in Cartesian system is:

$$\frac{\partial}{\partial x}(\rho u\phi)+\frac{\partial}{\partial y}(\rho v\phi)=\frac{\partial}{\partial x}\left(\Gamma_\phi\frac{\partial\phi}{\partial x}\right)\frac{\partial}{\partial y}\left(\Gamma_\phi\frac{\partial\phi}{\partial y}\right)+S_\phi \quad (1)$$

In this equation Γ_ϕ is the exchange coefficient of ϕ diffusion and S_ϕ is an accumulation of source terms not explicitly represented by the remaining terms in the equation. The governing equations used in the present paper are given in Table 1.

In the solar still, the natural convection is driven by the buoyancy force F_b that appears in the source term of y momentum equation. This

Table 1
Equations solved and definitions of exchange coefficients and source terms in general transport equation (1)

Equation	ϕ	Γ_ϕ	S_ϕ
Continuity	1	0	0
x momentum	u	μ	$-\frac{\partial p}{\partial x}+\frac{\partial}{\partial x}\left(\mu\frac{\partial u}{\partial x}\right)+\frac{\partial}{\partial y}\left(\mu\frac{\partial v}{\partial x}\right)$
y momentum	v	μ	$-\frac{\partial p}{\partial y}+\frac{\partial}{\partial y}\left(\mu\frac{\partial v}{\partial y}\right)+\frac{\partial}{\partial x}\left(\mu\frac{\partial u}{\partial y}\right)+F_b$
Temperature	T	$\frac{\mu}{\mathrm{Pr}}$	0

force per unit volume can be given in terms of the thermal expansion coefficient β by:

$$F_b = \rho_0 g\beta(T - T_0) \tag{2}$$

where ρ_0 and T_0 are the reference density and temperature, respectively.

2.2. Simplifying assumptions

The following assumptions were proposed to facilitate the study of the complicated real flow in the solar still:

- Steady-state flow
- Constant temperatures on all the boundaries
- Evaporation of the water is not included
- Mixture of air and water vapour (humid air) exists in the still
- Variable properties for the thermophysical quantities.

The calculation method for the variable properties of the humid air is mentioned in the appendix.

2.3. Boundary conditions

The closure provided by these equations is completed by the specification of boundary conditions over the whole perimeter of the solution domain. In the present study, the associated boundary conditions (Fig. 1) can be simply stated as:

Glass surface: $u = v = 0,\ T = T_g = 293$ K

Front and back surfaces: $x = 0$ and $x = L$,
$u = v = 0,\ T = T_g = 293$ K

Water surface: $y = 0,\ u = v = 0,\ T = T_w = 363$K

The steady state temperatures of the glass T_g, and the water T_w were selected from experimental measurements of Rayan et al.[5].

2.4. Numerical procedure

The time-averaged equations of conservation of mass and momentum are discretized by a finite-difference method. The interpolation to determine grid's face values of the unknowns is accomplished by the Power–Law Differencing Scheme of Patankar [4]. The SIMPLER algo-

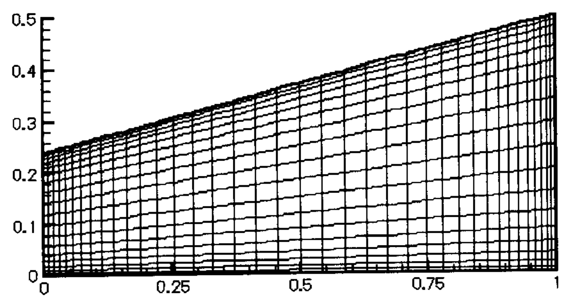

Fig. 2. Non-orthogonal grid (40×20 grids).

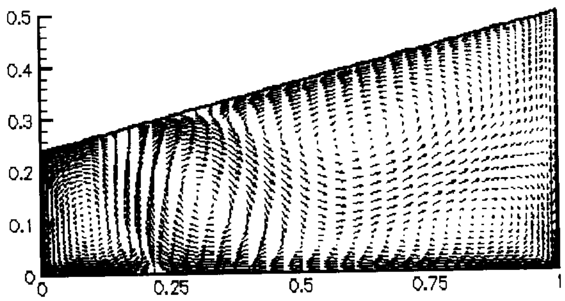

Fig. 3. Velocity vector contours in the solar still.

rithm [4] is used for the pressure–velocity coupling and the line-by-line solution method for solving the linearized equations. Successive iterations were performed until the summation of the residuals of the solved variables becomes less than 10^{-4}.

2.5. Grid size distribution

The variations in temperature near the surfaces have its role in the distribution of the temperature in the still. Therefore, a fine grid distribution is preferable near the surfaces and a coarse one in the core. The refinement of the grid near the vertical walls of the still for N grids in the x–direction was achieved using the following transformation [1]:

$$x = L \cdot \frac{(\beta+2\alpha)[(\beta+1)/(\beta-1)]^{(\bar{x}-\alpha)/(1-\alpha)} - \beta + 2\alpha}{(2\alpha+1)\left\{1+[(\beta+1)/(\beta-1)]^{(\bar{x}-\alpha)/(1-\alpha)}\right\}}, \quad (3)$$

$$\bar{x} = 1/N, 2/N, \ldots\ldots 1$$

A similar one was used for the stretching near the upper and lower surfaces. The resulting grid is illustrated in Fig. 2. with $N = 40$, $\alpha = 0.5$ and $\beta = 1.1$.

Various grid sizes were used to assess numerical accuracy. Grid sizes of 40×20; (Fig. 2); 45×30 and 50×40 were used. The grid independent solution was achieved by the 45×30 grids. However, to ensure grid size independence the finer 50×40 grids were used for all computations.

3. Numerical results and discussion

Fig. 3 presents the contours of the velocity vectors. The numerical results indicate clearly the existence of several circulation zones for the given geometry. The convection is connected to the mechanism of flow in the cavity. The optimum cavity will be the cavity that enhances the convection. The results show a large circulation zone expanded to cover more than 50% of the cross-section area. There is a reverse velocity adjacent to the inner surface of the glass cover. The productivity of the solar still depends on the sliding of the condensate on the inner cover surface to the collector channel. The existence of reverse velocity will certainly the cause the settlement of some drops back to the basin, which will result in reduction of the productivity. This phenomenon has been experimentally observed [5].

The temperature distribution is presented in Fig. 4. The isotherms plot show that the change of the temperature is very rapid beside the walls. The regions with highest temperatures exist in the narrow part of the still, while in the rest core part, the temperature is less by about 5K.

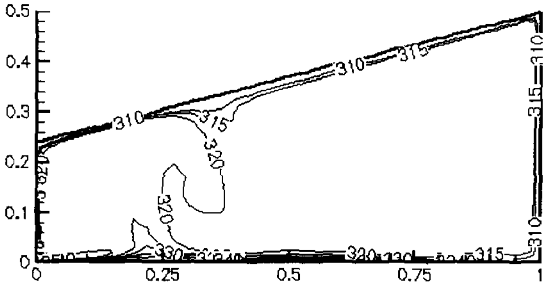

Fig. 4. Isotherms distribution (in Kelvin) in the solar still.

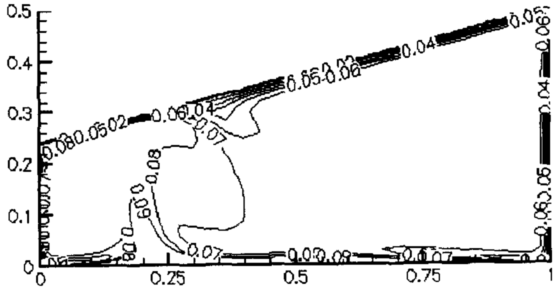

Fig. 5. Iso-humidity lines in the solar still.

The numerical calculation has also shown a temperature concentration in the region of contact and interaction between two circulation zones, Fig. 4.

Fig. 5 shows the distribution of constant humidity ratio lines. As mentioned previously, the narrower zone has a greater value of humidity ratio which increases the condensation of the water vapour in that region. It is similar to a stagnation wall with adverse velocity. This detail shows clearly the importance of numerical calculation before the geometrical configuration of the still.

4. Conclusions

Based on the present investigation, the following conclusions and recommendations are offered:

1. The finite-difference simulation of the variable property natural convection has proved to be a valuable tool in predicting the flow pattern inside the solar still.
2. The theoretical result shows clearly the importance of still dimensions, several circulation zones are observed. In the lower part, a reverse velocity is observed. The direction of this velocity is opposite to the direction of descending water droplet on the inner side of the glass cover.
3. A zone of high temperature concentration is recorded, corresponding to adverse velocity fields. This zone is like stagnation zone.

Further investigation is required in order to study the efect of the different parameters such as the inclination angle of the glass cover.

5. Symbols

a,b,c,d — Constants, Eq. (A2)
C_p — Specific heat capacity at constant pressure, J/kg.K
F_b — Buoyancy force, N
g — Acceleration of gravity, m^2/s
H — Height of the back wall of the still, m
k — Thermal conductivity, W/m.°C
L — Length of the still, m
M — Mean molecular weight of the humid air, kg/kmol
M_{air} — Molecular weight of air, kg/kmol
M_v — Molecular weight of water vapour, kg/kmol
N — Number of grids in the x-direction
Pr — Prandtl number, $C_p\mu/k$
p — Static pressure, Pa
p_{air} — Partial pressure of dry air, Pa
p_v — Partial pressure of water vapour, Pa
R — Universal gas constant, 8314 J/kmol.K

r_i — Volumetric fraction of the i-th gas componen' in the mixture
S_ϕ — Source term
T — Static temperature, K
u — x-direction velocity component, m/s
V_i — Partial volume of the i-th gas component in the mixture
V_{mix} — Volume of the mixture, m^3
v — y-direction velocity component, m/s
x — Horizontal coordinate direction
y — Vertical coordinate direction

Greek

β — Thermal expansion coefficient, l/K
Γ_ϕ — Exchange coefficient
θ — Slope of the glass cover, °
μ — Laminar dynamic viscosity, Pa.s
ρ — Fluid density, kg/m^3
ϕ — Dependent variable
ω — Humidity ratio, kg H_2O/kg dry air

Subscipts

a — atmosphere
air — air
g — glass cover
mix — mixture
o — reference
v — water vapour
w — water

References

[1] D.A. Anderson, J.C. Tannehill and R.H. Pletcher, Computational Fluid Mechanics and Heat Transfer, Hemisphere Publishing Corporation, New York, 1984.
[2] J.H. Keenan and F.G. Keyes, Thermodynamic Properties of Steam, John Wiley and Sons, New York, 1936.
[3] A. Palacio and J.L. Fernandez, Solar Energy, 50 (1993) 469.
[4] S.V. Patankar, Numerical Heat Transfer and Fluid Flow, McGraw-Hill New York, 1980.
[5] M.A. Rayan, A.E. Kabeel and A.A. Risha, Proc., Third Int. Water Technology Conf., Alexandria, (1998) 343.
[6] D.Y. Shang and B.X. Wang, Int. J. Heat Mass Transfer, 33 (1990) 1387.
[7] D.Y. Shang and B.X. Wang, Int. J. Heat Mass Transfer, 34 (1991) 749.
[8] G.N. Tiwari and V.S.V. Bapeshwara Rao, Desalination, 49 (1984) 231.
[9] G.N. Tiwari, K. Mukherjee, K.R. Ashok and Y.P. Yadav, Desalination, 60 (1986) 191.
[10] S. Toyama, T. Aragaki, K. Murase and K. Tsumura, Desalination, 45 (1983) 101.

Appendix

In the solar still, mixtures of dry air and water vapour, humid air, is encountered. At comparatively low pressures (close to atmospheric), both the dry air and the water vapour contained in it can be regarded as ideal gases. Denoting the partial pressure of dry air by p_{air}, the partial pressure of water vapour by p_v and then the pressure of the humid air; in accordance with Dalton's law; is given by:

$$p = p_{air} + p_v \tag{A1}$$

The partial pressure of water vapour at any temperature from 10°C to 150°C is given by the following equation due to Keenan and Keyes [2]:

$$p_v = 164960.72 \times 10^{-\left[X\left(a+bX+cX^3\right)\right]/\left[T\left(1+dX\right)\right]} \tag{A2}$$

where $X = 647.27 - T$, $a = 3.2437814$, $b = 5.86826 \times 10^{-3}$, $c = 1.1702379 \times 10^{-8}$, and $d = 2.1878462 \times 10^{-3}$. ($p_v$ is in mm of Hg and T is in degrees K).

Denoting the partial volume of the i-th gas component by V_i, then the volume fraction of the given component r_i is defined as the ratio between the partial volume V_i and the volume of the mixture V_{mix}. The partial volume is determined from Boyle's law ($p_{mix} V_i = p_i V_{mix}$), thus:

$$r_i = \frac{V_i}{V_{mix}} = \frac{p_i}{p_{mix}} \quad \text{(A3)}$$

Consequently, the volumetric fractions of the dry air and the water vapour can be expressed as the ratio of the partial pressure of the component in the mixture to the total mixture pressure:

$$r_{air} = \frac{p_{air}}{p} \text{ and } r_v = \frac{p_v}{p} \quad \text{(A4)}$$

Dry atmospheric air consists of 21% oxygen and 78% nitrogen by volume plus small amounts of other gases.

The mean molecular weight of the humid air is:

$$M = M_{air}\, r_{air} + M_v\, r_v \quad \text{(A5)}$$

where the molecular weights of air M_{air} = 28.96 kg/kmol and water vapour M_v = 18.016 kg.kmol

The equation of state for humid air is; (the universal gas constant R = 8314 J/kmol.K):

$$\frac{p}{\rho} = \frac{8314T}{M_{air} - (M_{air} - M_v)\frac{p_v}{p}} \quad \text{(A6)}$$

Thus, the density can be obtained:

$$\rho = \frac{28.96p - 10.94p_v}{8314T} \quad \text{(A7)}$$

The humidity ratio is the mass (in kg) of water vapour contained in the air–vapour mixture per kg of dry air:

$$\omega = \frac{0.622p_v}{p - p_v} \quad \text{(A8)}$$

The Prandtl number ($C_p\mu/k$) of the humid air depends mainly on the temperature and the humidity ratio. The three physical quantities, C_p, μ and k are evaluated as follows:

The specific heat capacity at constant pressure for the humid air is given by:

$$C_p = r_{air}\frac{M_{air}}{M}C_{p\,air} + r_v\frac{M_v}{M}C_{p\,v} \quad \text{(A9)}$$

The specific heats of water vapour C_{pv}, and dry air (nitrogen and oxygen) $C_{p\,air}$ are obtained using polynomials of the form:

$$C_{p,i} = \frac{R}{M_i}(C_{1i} + C_{2i}T + C_{3i}T^2 + C_{4i}T^3 + C_{5i}T^4) \quad \text{(A10)}$$

The constants of the polynomials are obtained from standard thermochemical tables and are listed in Table 2.

The dynamic viscosity of the humid air varies little from that of dry air at normal atmospheric pressure, and the thermal conductivity is essentially identical. For small humidity ratios, $\omega < 0.2$, the decreases in the dynamic viscosity and thermal conductivity could be neglected. Following Toyama et al. [10] these two thermophysical quantities for the dry air have been evaluated using the expressions given below:

$$k = 0.0244 + 0.7673 \times 10^{-4}(T - 273.15) \quad \text{(A11)}$$

$$\mu = 1.718 \times 10^{-5} + 4.62 \times 10^{-8}(T - 273.15) \quad \text{(A12)}$$

Table 2
Constants in the polynomials for heat capacity and the molecular weights for water vapour, nitrogen and oxygen (T < 1000 K)

Gas	C_1	$C_2 \times 10^{-3}$	$C_3 \times 10^{-6}$	C_4	C_5	M
H_2O	4.0701	1.1084	4.1521	-2.9637×10^{-9}	8.0702×10^{-13}	18.0
N_2	3.6748	-1.2081	2.3240	6.3218×10^{-10}	-2.2577×10^{-13}	28.0
O_2	3.6256	-1.8782	7.0555	-6.7635×10^{-9}	2.15556×10^{-12}	32.0